

Article

4T Analog MOS Control-High Voltage High Frequency (HVHF) Plasma Switching Power Supply for Water Purification in Industrial Applications

T. N. V. Krishna ^{1,†}, P. Sathishkumar ^{1,†}, P. Himasree ¹, Dinah Punnoose ², K. V. G. Raghavendra ¹, Himanshu ¹, Bandari Naresh ¹, R. A. Rana ¹ and Hee-Je Kim ^{1,*}

¹ School of Electrical Engineering, Pusan National University, Busandaehak-ro 63 beongil 2, Busan 46241, Korea; vamsik.tirumalasetty@gmail.com (T.N.V.K.); sathishnano2013@gmail.com (P.S.); himabindu1685@gmail.com (P.H.); raghavendra999@gmail.com (K.V.G.R.); himanshuhimanshu820@gmail.com (H.); naresh1.bandari@gmail.com (B.N.); ronak.eleindia@gmail.com (R.A.R.)

² Department of Computer Science and Engineering, Hindusthan Institute of Technology and Science, Chennai 603103, India; dinahpunnoose@gmail.com

* Correspondence: heeje@pusan.ac.kr; Tel.: +82-51-510-2364

† Both authors equally contributed to this work.

Received: 7 September 2018; Accepted: 8 October 2018; Published: 11 October 2018



Abstract: High-power plasma power supply is very useful for many industrial and medical applications. Plasma is generated artificially in the laboratory or industry by applying the electric or magnetic field. In this manuscript, we presented the simple 4T analog MOS control high voltage high frequency inverter circuit as a plasma power supply using modulation index technique. The presented plasma power supply operated at 25 kHz frequency and 10 kV peak to peak voltage. It generates a 0 V to 10 kV controllable electric field. The generated electric field is applied and produces plasma, which can be used for many industrial applications. A 10 kV to 5 kW plasma power supply has been practically developed based on the proposed topology and experimentally tested and, additionally, excellent output power conversion efficiency is achieved. From these results, the 4T analog MOS control high voltage high frequency (HVHF) plasma switching power supply is verified.

Keywords: 4T analog MOS control; high frequency switching power supply; water purification; modulation index

1. Introduction

Plasma is an ionized gas, into which sufficient energy is provided to free electrons from atoms or molecules. It sometimes allow species, ions, and electrons to coexist [1]. The most important thing is that plasmas are the high common state of matter in the universe and even on earth. Plasma is a gas that has been energized to the point that some of the electrons break free from, but travel with, their nucleus. Gases can become plasmas in several ways, but all include pumping the gas with energy. A spark in a gas will create plasma. Plasma is an electrically inoffensive medium of unbound positive and negative particles. Although they are not ‘free’ in the sense of not experiencing forces. Moving charged particles generate an electric current within a magnetic field, and any movement of a charged plasma particle affects and is affected by the fields created by the other charges. In turn, this governs collective behavior with many degrees of variation [2,3].

Basically, plasma is generated artificially in the laboratory or industry by the application of an electric or magnetic field through a gas. Although there are several means for plasma generation, in all cases, there must be a plasma power source to produce and sustain it [4]. Plasma can apply a voltage,

and subsequently ionization can occur, as shown in Figure 1, which presents a discharge tube as a simple example. The potential difference and subsequent electric field pull the bound electrons toward the anode, while the cathode pulls the nucleus [5]. As the voltage is increased, the current stresses the material by increasing electric polarization. Once the polarization exceeds the dielectric limit, electrical breakdown occurs, where the material transforms from being an insulator to a conductor. The underlying fundamental process is called an avalanche, where collisions between electrons and neutral gas atoms produce more ions and electrons.

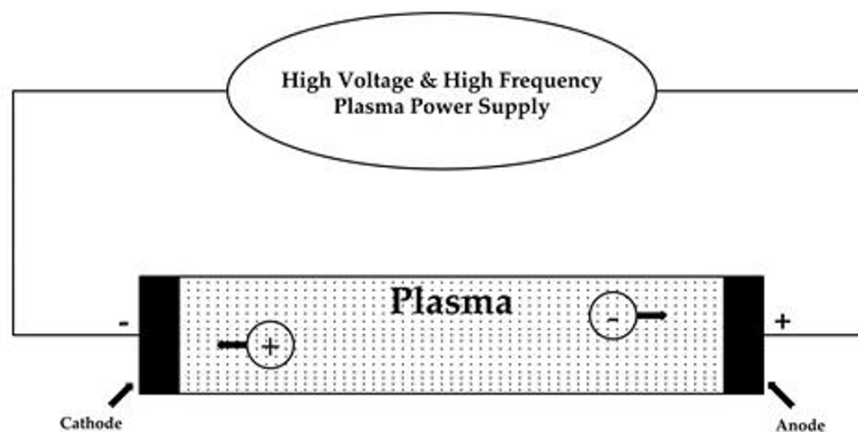


Figure 1. Simple representation of plasma discharge tube.

Plasma requires high voltage high frequency (HVHF) switching power supply as a source. HVHF is being used for many industrial applications [6–8], such as water purification, static charge removers, fluorescent tubes, plasma arc welding, plasma cutting, textiles, surface modification [9,10], biomedical applications [11–13], plasma displays, radicals, plasma needles [14], corona discharges [15], medical applications, and ozone generators [16]. Medical uses are an exciting new area for plasma applications that can be used in the treatment of diseases and cancer. In essence, the ozone generator is used for sterilization [17] and imprinting plastic and metal items, and involves the ionization of air. Ozone is produced in nature in two ways: corona discharge and ion propulsion method. A corona discharge in nature is called a lightning strike caused by a high voltage DC discharge of electricity. Ion propulsion is another interesting method in near future plasma applications, because it allows spacecraft to travel vast distances.

Various power sources, such as DC, RF, and microwave, are being developed in laboratories and industries to generate electrical current by applying very high voltage high frequency electric fields through a gas. On the other hand, the operation of plasma sources has different requirements according to the applications. Therefore, in most cases, to match with the application requirements, different voltages and different frequency pulsating DC systems are being developed for generating required electric field to produce electric current. In the present study, a high voltage high frequency plasma power supply was presented, which produces the essential plasma source for water purification in industrial applications [18–20]. In this design, we use a modulation index technique that controls the amplitude and frequency.

According to review [21], Weltmann and Woedtke designed the plasma source for sterilizing medical devices. They developed a high voltage and high frequency plasma source using a pulsed sinusoidal voltage of 10 kV/20 kHz. A high voltage and high frequency power supply was designed for an ozone generator, which is one of the plasma applications, for use in air and water disinfection [22]. This laboratory-built power supply using a high voltage ferrite transformer and a PLC microcontroller was used to energize a dielectric barrier discharge ozone generator. Cui juxia et al. designed a high voltage power supply for electro curtain applications [23]. The developed circuits achieved a high power factor, high efficiency, rapid fault response, and low ripple systems. For plasma torch

applications, a high power converter circuit was designed, including a rectifier and filter system, and a converter circuit was designed using ferrite material with high frequency and output voltage with a rapid time [24]. For plasma immersion ion implantation applications, they designed pulsed modulators with a high voltage system. A PLC-based pulse modulator and PLC driving system is presented, and the PLC system is very powerful for optimizing ion-implantation. The protection circuit was also designed for short circuits [25]. The other proposal is for surface treatment by plasma immersion ion implantation. This design consists of three basic circuits: pulse forming network, hard-tube pulsar, and Blumlein line [26].

The authors of [27] demonstrate the advantages of parallel and series configuration of flyback converters for pulsed power applications. Thus, the concept is to increase the voltage level and rise time of the generated pulses while emphasizing the modularity concept. There are two kinds of experimental sections that occurred, one is 4 kV output voltage and other is 20 kV output voltage, while the repetition rate of frequency is 1 kHz. On other hand, the authors of [28] demonstrate how the proposed topology operates independently from the load while preserving high repetition rate. The control algorithm is designed in a way that it can prevent from any possible faults and protect the system from the over-voltage. The designed system is between 1 kV and 3 kV with different circumstances. We presented high voltage high frequency plasma power supply with 10 kV, 5 kW, and 25 kHz; repetition rate of frequency is high. We presented both voltage and current protection circuits to prevent the system from having any issues. Mainly, this plasma power supply presents the line regulation circuit to maintain a stable output regardless of changes in the input voltage, load, or connected device.

In the work of [29], the experimentations have been conducted based on a high-voltage DC power supply and a high-voltage pulse generator for point-to-point and point-to-plane geometries. In addition to the employed geometry, the ambient also plays an important role on electric field formation. Thus, the electric field distribution was simulated for both aforementioned geometries in air–water medium. In this case, the high electric field strength for both geometries appears across the point electrode. This is because of the fact that the water conductivity makes the electric field distribution for both geometries almost similar. Here, the water conductivity was selected to be 200 $\mu\text{S}/\text{cm}$, the same as the tap water used in the experimentation phase. In this research paper, gas can produce an electric or a magnetic field in plasma. We presented the plasma power supply with 10 kV_{p-p}, which is applied to the plasma load for water purification. The pros of the design are simplicity, cost-efficiency, and quick purifying of the water. The cons of the system are heat, explosion risk, and its time-consuming nature.

The plasma has requirements based on the applications. For example, the helicon plasma will work at 13.56 MHz with radio frequency levels up to 120 kW; microwaves at 28 GHz, which requires up to 30 kW; and ion cyclotron heating operates at 7–9 MHz, which will work until 30 kW [30]. This paper presented a fully analog-controlled high voltage high frequency (HVHF) plasma switching power supply. The developed HVHF topology applies for water purification in industry. Water purification is the kind of removing dust particles, undesirable chemicals, suspended solids, and gases from water. The goal is to produce water for a specific purpose. Most water is disinfected for human consumption, but water purification may also be designed for a variety of other purposes, including fulfilling the requirements of medical, pharmacological, chemical, and industrial applications.

There are some plasma technologies that are regularly used for water purification, such as ozone, electron beam, and electrical discharge. We presented the electrical discharge technique, which generates ions and electrons with very high energy as active species. The active species will remove the dust particles and unwanted waste particles. Because of their physical and chemical properties, the substantial amount used for the electrodes affects the chemical process of plasma in water, necessitating a study of difference in electrode substantial in plasma discharge used in organic solution removal. The objective of this work is explained on water purification by plasma technology has been presented and experimentally verified. A plasma power supply with an output

voltage of 10 kV was connected to the plasma load to start the electrical discharge. In this design, the input of 200 V AC to 240 V AC is applied to the plasma power supply and will generate 10 kV_{P-P} alternating current. This high voltage of AC is connected to the plasma load, which is applied to the water. The effects of variable modulation index on the total harmonic distortion (THD) content of the resulting inverter output are studied.

The 10 kV, 5 kW presented 4T analog MOS control HVHF plasma switching power supply was developed in the laboratory and a generated high frequency electric field was applied, which produces the required electric power for plasma. Section 2 presents a detailed explanation of the HVHF power supply, which is a combination of diode bridge rectifier, high voltage and high frequency PWM inverter, high frequency transformer, filter design, and line-regulation. The modulation technique is explained in Section 3. The experimental setup of the HVHF power supply and practical work are reported in Section 4. The experiment results and discussion on the HVHF with the power conversion efficiency of design are presented in Section 5. Finally, Section 6 reports the conclusions on research and development of the system.

2. High Voltage High Frequency Plasma Power Supply

The block diagram of the HVHF plasma switching power supply is shown in Figure 2. A single phase AC source was applied as the input to the designed power supply. A diode full bridge rectifier circuit was designed as the initial stage of the plasma power supply. The circuit rectifies the 220 V AC voltage to DC output voltage [31–39], which can be adjusted from 0 V to 300 V. A high frequency inverter circuit was designed and located, following by the rectifier DC link capacitor, which receives the DC voltage from the rectifier and converts it to a high frequency pulsating DC output voltage. The full-bridge PWM topology with high switching frequency was developed as an inverter circuit for the designed plasma power supply. A high voltage and high frequency transformer was designed and placed at the output of the inverter side. The high frequency pulsating DC output was connected to the primary side of the transformer. The transformer was designed with a ferrite PL-13 U core that could transform 290–300 V to 10 kV high voltage. The secondary side of the transformer that transformed the high voltage was connected to the plasma source, which was designed with titanium, quartz tube, and metal.

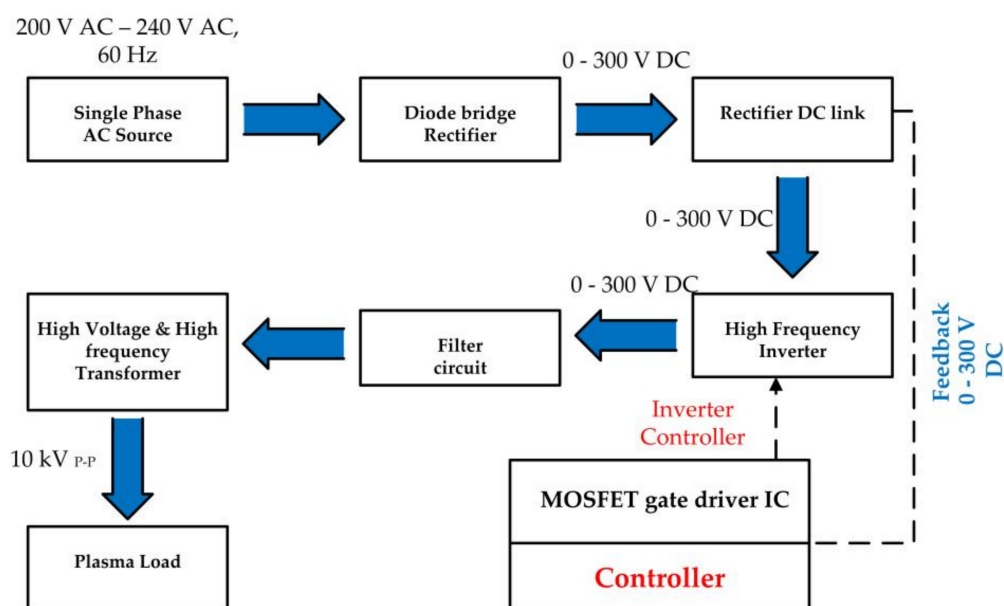


Figure 2. Block diagram of the high voltage high frequency (HVHF) plasma switching power supply.

Figure 3 shows the schematic diagram of 4T analog MOS control plasma switching power supply. The single phase AC voltage was applied to the circuit. The GBJ2506 bridge rectifier was used along with the DC link capacitors. The designed rectifier full bridge consisted of four diodes that were arranged as shown in Figure 3.

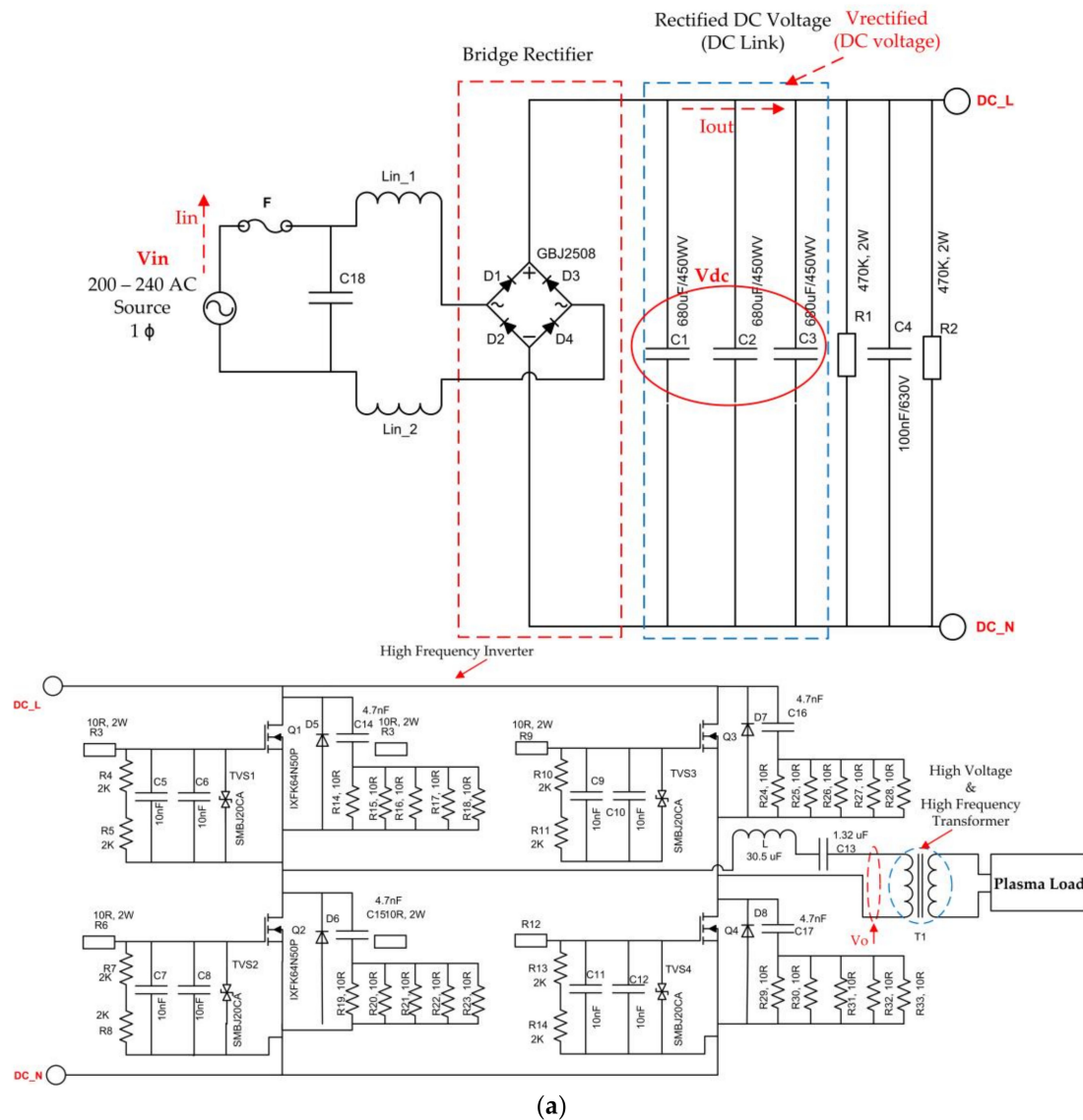


Figure 3. Cont.

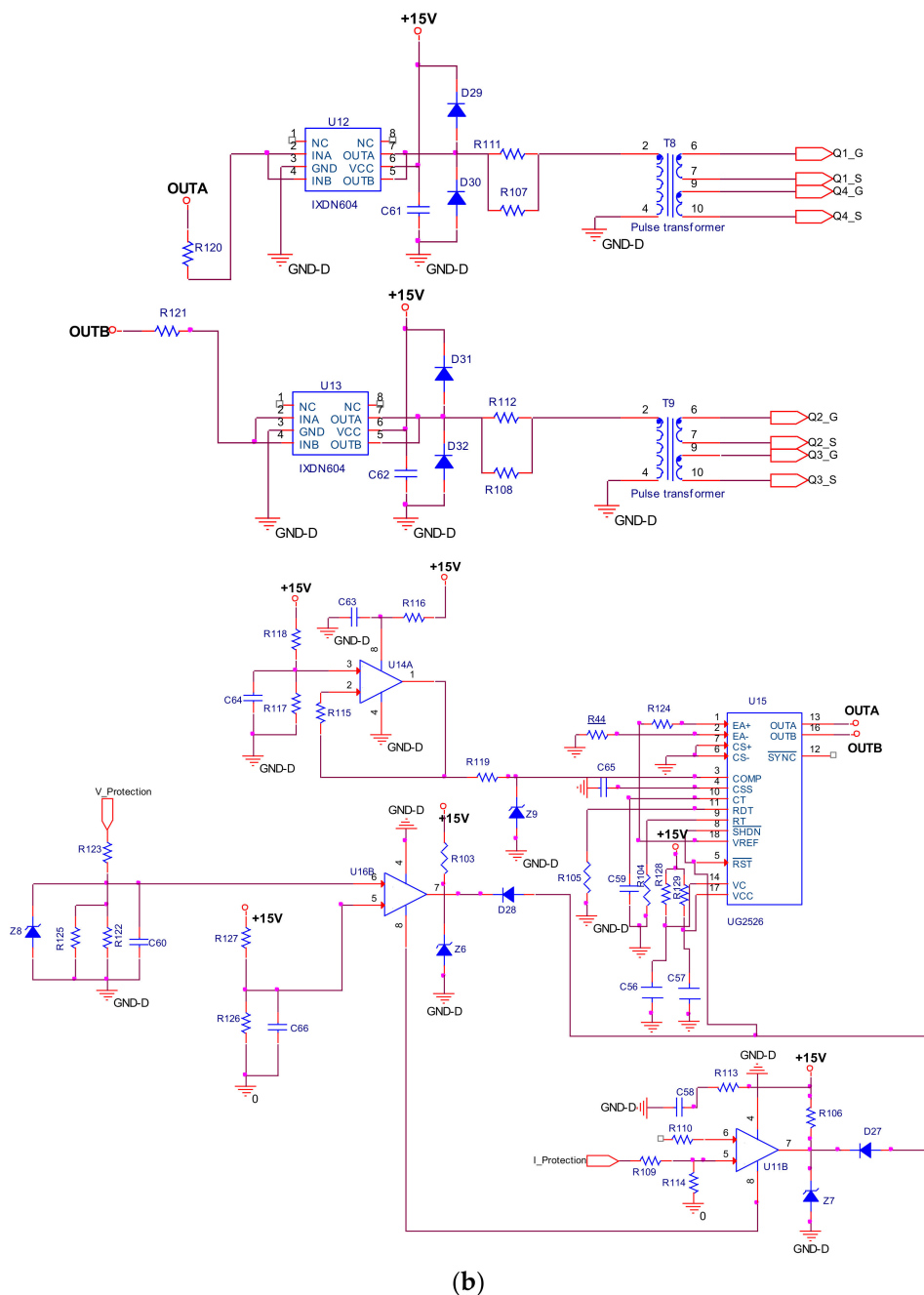


Figure 3. Schematic diagram of 4T analog MOS control HVHF plasma switching power supply. (a) Power circuit of HVHF plasma. (b) MOSFET driver circuit of the PWM inverter.

2.1. High Voltage High Frequency PWM Inverter

A high switching frequency high power PWM inverter circuit was designed and placed followed by the rectifier of the plasma power supply, as shown in Figure 3. The IXFK64N50P MOSFET was used as a switching device in the PWM full bridge inverter. The chosen MOSFET allowed a 500 V and 64 A maximum. This has a lower drain source resistance (85 m ohms) and fast intrinsic diode. An inverter driver circuit was designed along with a regulating pulse width modulator IC (UC2526) to operate the full bridge PWM inverter as shown in Figure 3b. The driver circuit generates two complementary PWM signals operating at 25 kHz with a 0.5 μ s dead band. The MOSFET driver IXLN604SIA is dual high speed gate drivers are especially well suited for driving the MOSFETs and IGBTs. Each of the two outputs can source and sink 4 A of peak current while producing voltage rise and fall times of less than

10 ns. The input of each driver is virtually immune to latch up, and proprietary circuitry eliminates cross conduction and current shoot through. The pulse width modulator IC UC2526 is designed for fixed frequency. When the Q1, Q4 MOSFET switches ON and the Q2, Q3 MOSFET switches off, a positive DC voltage is obtained at the output. When the Q2, Q3 MOSFET switches ON and the Q1, Q4 MOSFET switches off, a negative DC voltage is obtained at the output. The MOSFET switches are switched alternately with a controlled duty ratio to convert input DC voltage into high frequency AC voltage suitable for exciting the plasma load. The PWM driver circuit was designed using 4 A dual low side ultrafast MOSFET drivers (IXDN604SIA). The 25 kHz inverter circuit can generate up to a 640 V peak to peak square wave voltage. The designed plasma power supply consisted of an over voltage, over current, and over temperature protection circuit. These protection circuits shut down both the phase controller and PWM controller in any unusual circumstances.

The switching sequence is designed so that switches Q1 and Q4 are ON for the time duration $0 \leq t \leq T_1$ and switches Q2 and Q3 are ON for the time duration $T_1 \leq t \leq T_2$. When switch Q1 and Q4 are turned ON,

$$V_{out} = \frac{V_i}{2} \quad (1)$$

When switches Q2 and Q3 only are turned ON,

$$V_{out} = -\frac{V_i}{2} \quad (2)$$

The waveform of the output voltage and switch currents for a load are shown in Figure 1.

The rms value of the output voltage is V_{out} is

$$V_{out, rms} = \frac{1}{T_1} \int_0^{T_1} \frac{V_i^2}{4} dt = \frac{V_i}{2} = \frac{V_i}{2} \quad (3)$$

The instantaneous output voltage (V_{out}) is rectangular in shape. The instantaneous value of V_{out} can be expressed in Fourier series as follows:

$$V_{out} = \frac{a_0}{2} + \sum_{n=1}^{\infty} a_n \cos(n\omega t) + b_n \sin(n\omega t) \quad (4)$$

As a result of the quarter wave symmetry along the time axis (Figure 4d), the values of a_0 and a_n are zero. The value of b_n is given by

$$b_n = \frac{1}{\pi} \int_{-\frac{\pi}{2}}^0 -\frac{V_i}{2} d(\omega t) + \int_0^{\frac{\pi}{2}} \frac{V_i}{2} d(\omega t) = \frac{2V_i}{n\pi} \quad (5)$$

Substituting the value of b_n from Equation (5) into Equation (4),

$$V_{out} = \sum_{n=1,3,5,\dots}^{\infty} \frac{2V_i}{n\pi} \sin(n\omega t) \quad (6)$$

The current through the load (i_L) is given by

$$i_L = \sum_{n=1,3,5,\dots}^{\infty} \frac{1}{R} \frac{2V_i}{n\pi} \sin(n\omega t) \quad (7)$$

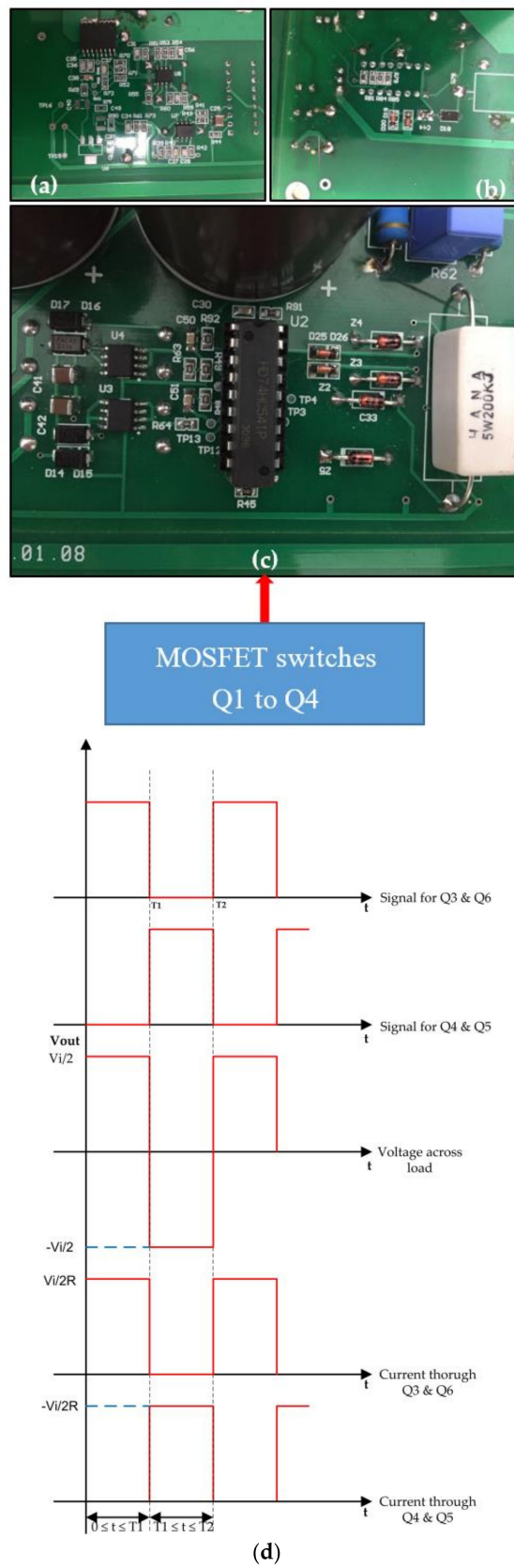


Figure 4. HVHF plasma power source driver and protection circuits. (a,b) Voltage and current protection circuit; (c) MOSFET driver circuit; (d) current and voltage waveforms of PWM inverter.

2.2. Filter Design

This filter contains two components. An inductor connected in series with the capacitor, which is why this low pass is also referred to as an LC low pass filter. The primary side of transformer voltage V_o is employed parallel to the capacitor. The output frequency of the plasma power supply is 25 kHz. The inductor L is more approachable to the surge of frequency. As the frequency rises, the inductive reactance of the coil X_L increases, while the capacitance X_C of the capacitor drops.

The formula for computing the LC filter is

$$LC = \frac{1}{1 - \omega^2 LC} \quad (8)$$

In this design, L is the inductor and C is the capacitor.

The inductive resistance X_L rises with frequency while the capacitive reactance X_C is inversely proportional to it and it falls down as the frequency increases. The cutoff frequency is the frequency at which $X_C = X_L$. Thus, at a frequency greater than the cutoff frequency, X_C is less than X_L . At a lower frequency, X_C is greater than X_L .

The cut-off frequency is

$$f_c = \frac{1}{2\pi\sqrt{LC}} \quad (9)$$

The L–C Circuit Damping Method

The loads connected to the PWM inverter circuit may damage the L–C filter circuit by providing some damping. The load effects on the L–C filter can be enlightened from the energy point of view.

The voltage (and current) that spins around inside L–C circuits can be greater than the initial voltage that ‘kick starts’ the alternating capacitor charge and discharge and inductor ‘discharge and charge’ (via its magnetic field). In an inductor, the voltage across it is proportional to the rate of change of current flowing through it.

Or

$$V = L \times \left(\frac{d(I)}{dt} \right) \quad (10)$$

The constant of proportionality, L , is the inductance that we associate with the coil. Thus, a rapidly discharging capacitor connected in parallel with the inductor can increase voltage level higher than the initial voltage across the capacitor.

2.3. High Voltage High Frequency Transformer

A high voltage high frequency step-up transformer [40] was designed in the laboratory, as shown in Figure 5. The transformer step-up the inverter output voltage to a 10 kV peak to peak voltage and achieve galvanic isolation. A 100 nF capacitor is connected as a high pass filter between the inverter output and the primary winding of the high voltage transformer. It obtains the sine wave current waveform from the square wave voltage. The secondary side of the transformer output was connected to a quartz tube (plasma source), which was made of metal and titanium. The three high voltage capacitors were connected in parallel as a DC link with a value of 2040 μ F, 450 V.

The necessity of the transformer is mainly for a high voltage value at the secondary side, a specific shape for industrial applications. The high voltage high frequency transformer was designed for the plasma power supply, and has the following electrical specifications: output voltage $V_{out} = 10$ kV; output power $P_{out} = 5$ kW. As per design, high switching frequency will decrease the height and size of the transformer. However, further reduction by higher frequency switching cannot be achieved because of the insulation requirement. The natural resonant frequency of the high voltage transformer is also a restriction. Additionally, high frequency switching will require high driving power. As a compromise, $f_s = 25$ kHz is selected as the switching frequency.

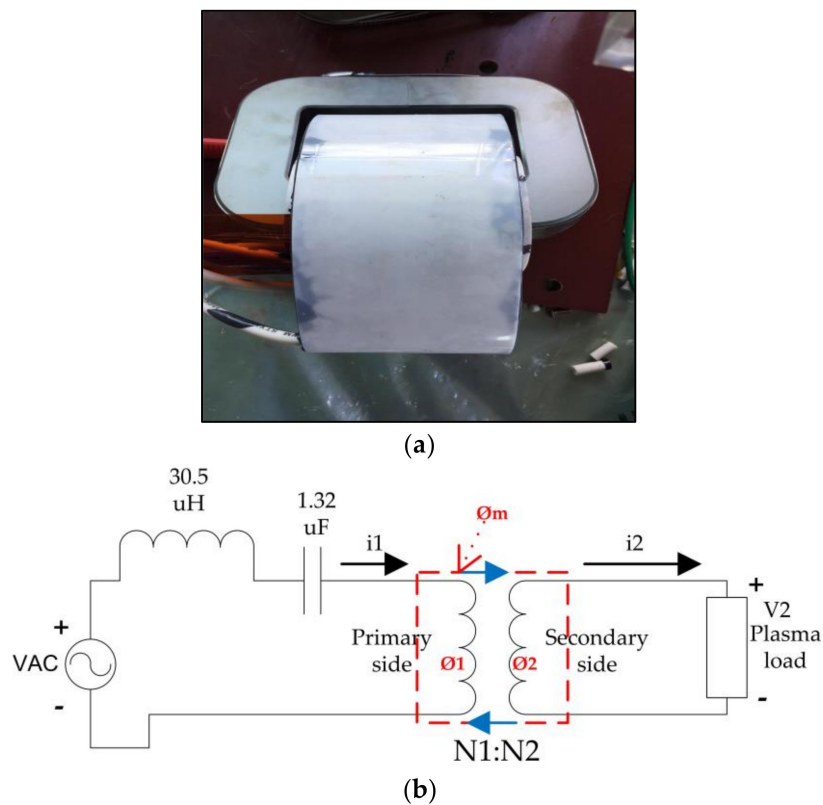


Figure 5. (a) High voltage high frequency transformer; (b) transformer equivalent circuit.

2.3.1. Turns Ratio

The DC link voltage is approximately 300 V DC, which is obtained by the rectifier. The output voltage is 10 kV. So the output–input ratio should be 33.33. Both the turn’s ratio of the transformer and plasma power supply contribute to the final voltage boost. Thus, in practice, the step-up coefficient of the plasma power supply is used as design margin and the turn’s ratio of the high voltage transformer is selected as 33.33.

2.3.2. Magnetic Selection

Power ferrites are employed as the magnetic material due to the high resistivity and low eddy current losses under high frequency. PL-13, UU120 is designated to accommodate the big winding turns and to fulfill the insulation requirement.

The turn’s number of the primary and the secondary side winding, n_1 and n_2 , can be calculated by (11) and (12), respectively, which yields $n_1 = 23$, $n_2 = 770$.

$$n_1 = \frac{V_i \times 10^4}{4B_{max} A_e F_s} \tag{11}$$

$$n_2 = 33.33 * n_1 \tag{12}$$

2.3.3. Wire and Wiring Design

The secondary winding plays a main role in the output voltage side. In practice, the secondary winding is wounded into five slots, each slot contains five layers. This assembly can limit the voltage across each slot and decrease the layer-to-layer voltage. Primary side used Ritz wire and secondary side high voltage Copper wire is used and results in a small leakage inductance. Considering the skin effect and the current value, the wire specifications and the current density are as follows: primary

winding—0.2 mm Ritz wire, 3 A/mm²; Secondary winding—AWG16 high voltage cable copper wire, 1 A/mm².

Primary and secondary windings have resistances, which means that the source voltage VAC is not the same as the induced primary voltage e_1 ; that is, $VAC \neq e_1$. Similarly, $V_2 \neq e_2$. The source voltage of primary side of transformer is coming from inverter output side. In deriving the equivalent circuit for the two-winding transformer of Figure 5b, the characteristics of an actual transformer described earlier need to be modeled.

Consider the primary circuit. A voltage equation around the loop may be written as

$$VAC = R1i1 + N1 \frac{d\lambda_1}{dt} = R1i1 + N1 \frac{d\Phi_1}{dt} \quad (13)$$

where

R1 is the resistance at the primary side

N1 is the number of primary windings

2.4. Advantages and Disadvantages of the Circuit

Advantages:

- The power supply circuit has a smaller size.
- It is lightweight.
- It has excellent power conversion efficiency from 75% to 85%.
- This design has high output range.
- Less heat produced in plasma power supply design.
- Simple application.

Disadvantages:

- This design has only one output range.
- It causes harmonic distortion.
- High frequency noise.
- More complex.

3. Modulation Technique

There are some differences between amplitude modulation index and frequency modulation index. The deviations of amplitude modulation index are values used are 0.3 to 1.0 with 0.1 increments. The reference frequency signal f_r describes the inverter output frequency, with its peak amplitude and control the modulation ratio m_a . The PWM inverter has constant DC input for generating certain frequency. The modulation index m_a , also known as the amplitude modulation ratio, is well-defined as (14) [41–43].

$$m_a = \frac{V_r}{V_c} \quad (14)$$

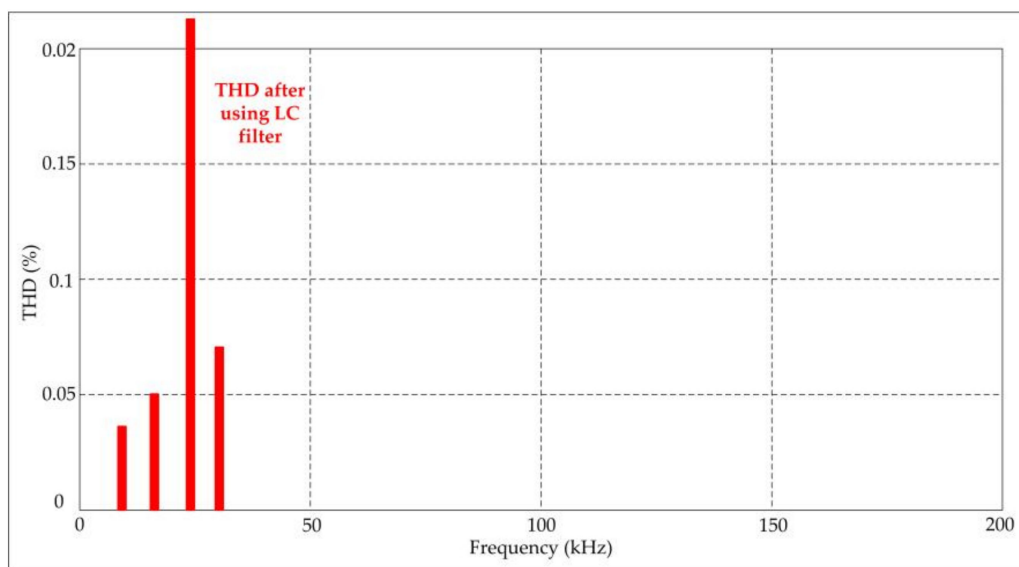
The variation of m_a can be produced by changing in the modulation signal. The effect of m_a on the total harmonic distortion (THD) of the inverters are illustrate in Table 1.

In addition, the results of a single phase PWM inverter are illustrated in Figure 3 respectively. The effect of modulation index on THD of the inverter before using a filter is given in Table 1. It can be seen that the least value of THD equals 2.08% is at modulation index m_a equals 0.9.

The outcome of a filter on the THD and the output voltage waveform are presented in Figure 6 respectively.

Table 1. Effect of modulation index on total harmonic distortion (THD) of the PWM inverter before using filter.

m_a	THD%
0.3	7.45%
0.4	9.74%
0.5	5.13%
0.6	6.03%
0.7	3.37%
0.8	3.42%
0.9	2.08%
1	2.81%

**Figure 6.** Effect of total harmonic distortion (THD) frequency modulation index.

4. Experimental Setup

The proposed HVHF plasma power supply was verified by operating the 5 kW plasma source in a laboratory. The single phase 220 V AC, 60 Hz grid power was applied as an input to the HVHF switching plasma power supply. A variable AC source, which can vary the input voltage up to 240 V AC, was used to verify the input saturation. As illustrated, this switching power supply is based on PWM inverter topology. This topology uses a high voltage high frequency step-up transformer to boost the voltage up to 10 kV peak to peak. The low pass LC filter was connected in series with the primary side of the transformer to achieve a sine wave current from pulsating DC voltage. The repetition rate is can be used to adjust the power and to obtain high frequency sine waveform. The repetition rate is set to 25 kHz to generate symmetrical waveform and avoid transformer saturation. The plasma power source as a load for 10 kV, 5 kW high power systems, which was designed using metal and titanium.

Here, high voltage MOSFET (IXFK64N50P) is used as power switches. IXDN604SIA gate drive modules are used to drive the MOSFETs and provide the necessary isolation between the switching signal ground and the power ground. Table 2 presents the HVHF switching plasma power supply specifications.

Table 2. The 10 kV, 5 kW PWM inverter for plasma power source design specification.

Parameter	Ratings
Input voltage	200 V AC–240 V AC
power	5 kW
Output voltage	10 kV _{P-P}
Switching frequency	25 kHz
DC link capacitor	2040 μ F

5. Results and Discussion

The HVHF plasma switching power supply design and workings are discussed below based on the experimental results. The experiments are made by applying output voltage 10 kV peak to peak. To verify the circuit, the experiments were carried out with a variable AC voltage and different input power.

Figure 7 shows the shows the DC voltage converted from the single phase AC sine wave with different input power.

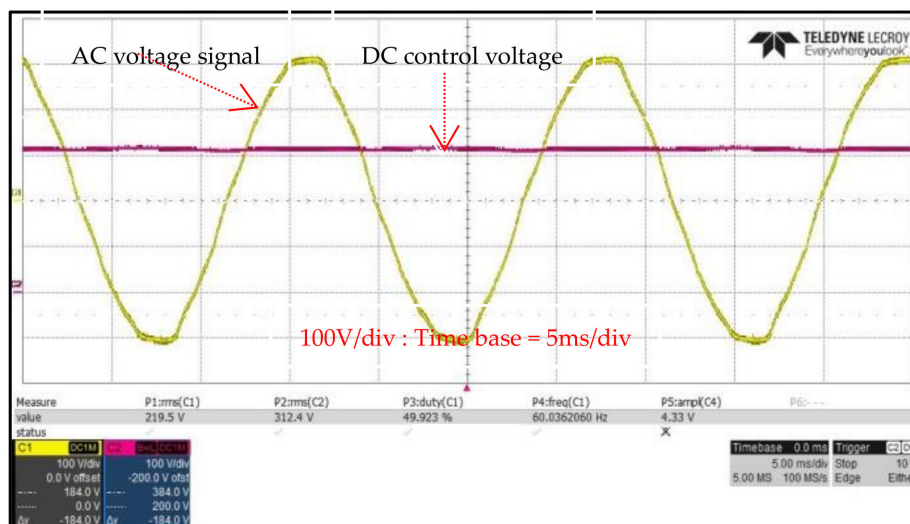


Figure 7. Full wave bridge rectifier resultant output waveform.

The high frequency PWM inverter output waveforms and gate signals are shown in Figure 8. The inverter output and high frequency square wave voltages were obtained from the DC input voltage from the bridge rectifier circuit. Figure 8a shows the two complementary 50% duty cycle PWM signals produced by the analog PWM controller. The two complementary PWM control signals synchronized with each other and consist of dead band, which avoids short circuit in full bridge. The controlled PWM signals were applied to the gate terminal of the MOSFET switches to switch the MOSFET on and off. Figure 8b presents the output voltage of inverter waveforms at various input voltages and Figure 8c presents output current waveform (5 A/div) of the inverter, respectively.

Figure 9 presents the HVHF plasma switching power supply output waveforms. Figure 9a shows the output voltage waveform of the transformer secondary side with the 10 kV. Figure 9b shows the output current waveform of inverter (5 A/div). The respective output current (500 mA/div) waveforms of the transformer secondary side that flow through the plasma source, as shown in Figure 9c. The output current of the inverter side was changed to a sinewave because of the series connected filter.

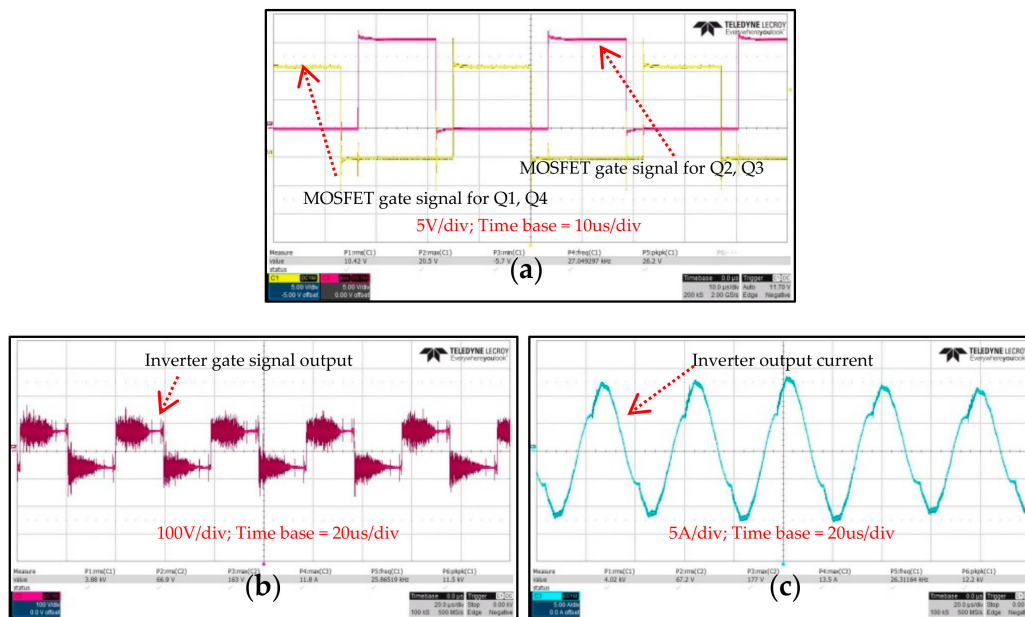


Figure 8. High frequency PWM inverter control and output waveforms. (a) MOSFET gate signals; (b) inverter gate signal output; (c) inverter output current.

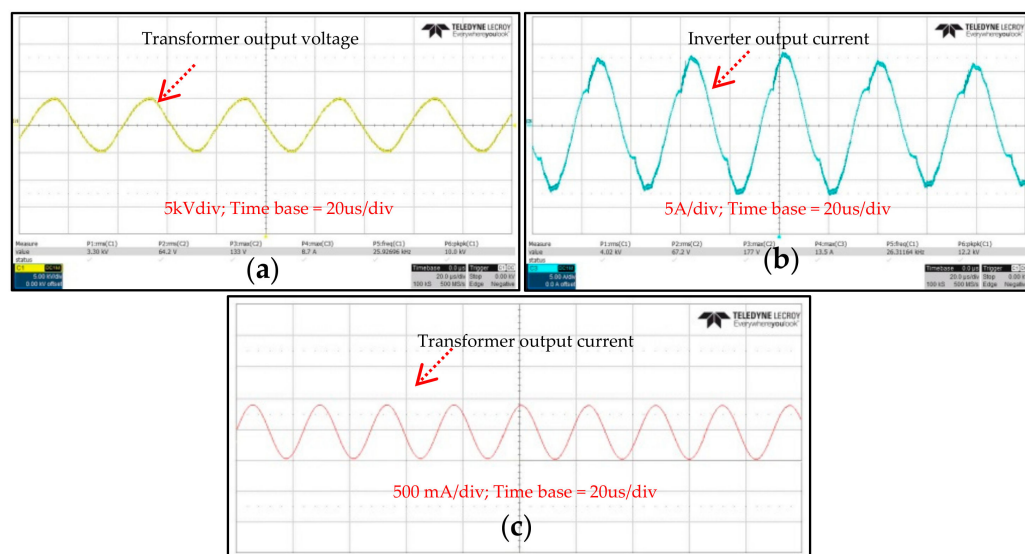


Figure 9. HVHF plasma switching power supply output waveforms. (a) Transformer output voltage; (b) Inverter output current; (c) Transformer output current.

Figure 10 shows the HVHF plasma power supply characteristics waveforms with and without regulation. Figure 10a presents the input voltage versus output DC controllable voltage and Figure 10b exhibits the input voltage versus output current. This comparison graph results are reported with and without regulation. When different AC input voltages were applied (200 V AC to 230 V AC) to the proposed HVHF plasma power supply, the DC output voltage also varied from 259 V to 310 V. The large saturation in output voltage will affect the plasma source and lead to damage. Therefore, a line regulation circuit was designed to avoid this saturation in the output. The low cost line regulation achieved low output changes (282 V to 291 V) for the input voltage saturation from 200 V to 240 V, as shown in Figure 10a. An output current of 407 mA to 484 mA was generated without regulation, whereas 455 mA to 472 mA was generated with regulation, as shown in Figure 10b. Therefore,

the proposed HVHF plasma power supply achieves a reliable output voltage and current for the plasma power source and assured safe operation.

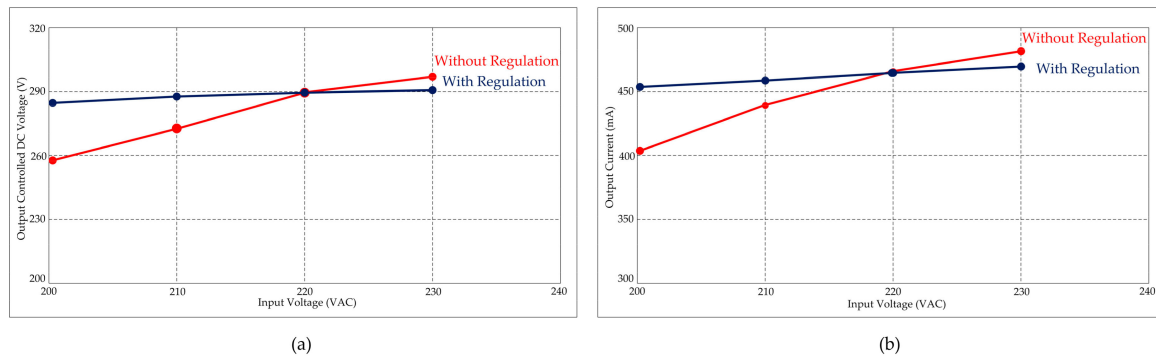


Figure 10. HVHF plasma switching power supply characteristic waveforms with and without regulation. (a) Input voltage vs. output DC controllable voltage; (b) input voltage vs. output current.

Efficiency Optimization

Figure 11 shows the power conversion efficiency. The MOSFET switches are used for high repetition rates (25 kHz), and excellent output power conversion efficiency is achieved from 75% to 85%, as shown in Figure 11. In order to examine the applied properties of the pulse generation arrangement, a set of prototypes was constructed. Basic experiments were plasma power supply design based on a topology depicted in Figure 3a (As in manuscript). The power supplied with an initial voltage is 200 VAC to 240 VAC and the DC initial voltage is 300 V DC. Capacitors were implemented using high voltage type with the value of $C1 = C2 = C3 = 680 \mu\text{F}$ each. The overall the output voltage of system is $10 \text{ kV}_{\text{p-p}}$. All the electrical waveforms were recorded using Teledyne Lecroy (350 MHz, 2 GS/s). Voltage pulse was measured by Teledyne Lecroy HighVoltage probe. Current was measured by a current monitor.

The capacitance is chosen at the outside side, namely $C13 = 1.32 \mu\text{F}$. The efficiency given below was calculated on the basis of energy balance of the DC link capacitors. This was measured using the half period voltage and current product.

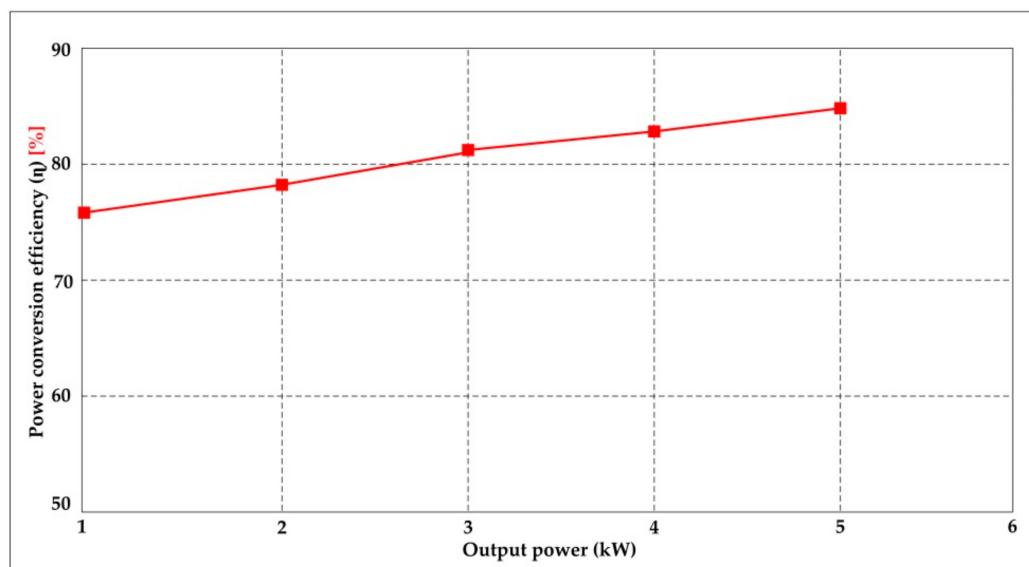


Figure 11. Power conversion efficiency.

6. Conclusions

A simple 4T Analog MOS control high voltage high frequency (HVHF) plasma switching power supply has been presented for water purification in industrial applications. The presented HVHF switching plasma power supply was controlled with fully analog control system and which is used by modulation index technique. The 10 kV, 5 kW plasma power source was designed and was used for operations for water purification in the industry. The presented plasma power supply operated at 25 kHz frequency and 10 kV peak to peak voltage. It generates 0 V to 10 kV controllable electric field. From the experimental results, the presented power supply is able to transmit 5 kW output AC power. Additionally, excellent output power conversion efficiency is achieved. This 4T analog MOS control HVHF switching plasma power supply has been practically developed based on the proposed topology and experimentally verified. The pros of the design are simplicity, cost-efficiency, quick purifying of the water. The cons of the system are explosion risk and its time-consuming nature. In future, a simple line regulation circuit with opto-isolated feedback is going to be designed for the 10 kV, 5 kW switching power supply, which comes with low cost, reliability, and high efficiency.

Author Contributions: T.N.V.K., P.S., and H.-J.K. conceptualized the idea of the research project. T.N.V.K., P.S., P.H., and D.P. designed the 10 kV, 5 kW high voltage high frequency plasma switching power supply with line regulation and protection circuit. T.N.V.K., P.S., and D.P. designed and developed the analog control and driver circuits. P.H., D.P., and K.V.G.R. developed PCB artwork for HVHF plasma power supply. H., B.N., and R.A.R. designed the high frequency transformer. T.N.V.K. and coauthors made the experimental setup and did the experiment. The data was analyzed and verified by H.-J.K. The paper was written by T.N.V.K. and P.S.

Funding: This research was supported by BK21PLUS, Creative Human Resource Development Program for IT Convergence.

Acknowledgments: This research was supported by Brain Korea 21 Center for Creative Human Resource Development Program for IT Convergence of Pusan National University.

Conflicts of Interest: The authors declare no conflict of interest.

References

1. Plasma. Available online: <https://www.britannica.com/science/plasma-state-of-matter> (accessed on 15 August 2018).
2. Sturrock, P.A. *Plasma Physics: An Introduction to the Theory of Astrophysical, Geophysical Laboratory Plasmas*; Cambridge University Press: New York, NY, USA, 1994; pp. 1–331, ISBN 978052144810-9.
3. Hazeltine, R.D.; Waelbroeck, F.L. *The Framework of Plasma Physics*; Westview Press: New York, NY, USA, 2004; pp. 1–314, ISBN 9780738200477.
4. Hippler, R.; Kersten, H.; Schmidt, M.; Schoenbach, K.M. *Low Temperature Plasmas: Fundamentals, Technologies, and Techniques*, 2nd ed.; Wiley-VCH: Greifswald, Germany, 2008; pp. 1–945, ISBN 9783527406739.
5. Chen, F.F. *Introduction to Plasma Physics and Controlled Fusion*, 2nd ed.; Springer: Berlin, Germany, 2013; pp. 1–421, ISBN 9780306413322.
6. Akiyama, H.; Sakugawa, T.; Namihira, T.; Takaki, K.; Minamitani, Y.; Shimomura, N. Industrial applications of pulsed power technology. *IEEE Trans. Dielectr. Electr. Insul.* **2007**, *14*, 1051–1064. [[CrossRef](#)]
7. Babaie, M.; Davari, P.; Zare, F.; Rahman, M.M.; Rahimzadeh, H.; Ristovski, Z. Effect of pulsed power on particle matter in diesel engine exhaust using a DBD plasma reactor. *IEEE Trans. Plasma Sci.* **2013**, *41*, 2349–2358. [[CrossRef](#)]
8. Scholl, R.A. *Power Supplies for Pulsed Plasma Technologies: State-of-the-Art and Outlook*; Advances Energy Industries, Inc.: Fort Collins, CO, USA, 1999; pp. 1–8.
9. Benedikt, J.; Focke, K.; Yanguas-Gil, A.; von Keudell, A. Atmospheric pressure microplasma jet as a depositing tool. *Appl. Phys. Lett.* **2006**, *89*. [[CrossRef](#)]
10. Fang, Z.; Yang, H.; Qiu, Y. Surface treatment of polyethylene terephthalate films using a microsecond pulse homogeneous dielectric barrier discharges in atmospheric air. *IEEE Trans. Plasma Sci.* **2010**, 1615–1623. [[CrossRef](#)]
11. Schamiloglu, E.; Barker, R.J.; Gunderson, M.; Neuber, A.A. Modern pulsed power: Charlie Martin and Beyond. *Proc. IEEE* **2004**, *92*, 1014–1020. [[CrossRef](#)]

12. Tehrani, A.H.; Davari, P.; Singh, S.; Oloyede, A. Sterilizing tissue-materials using pulsed power plasma. *J. Mater. Sci. Mater. Med.* **2014**, *25*, 1–12. [[CrossRef](#)]
13. Lu, X.; Jiang, Z.; Xiong, Q.; Tang, Z.; Pan, Y. A single electrode room temperature plasma jet device for biomedical application. *Appl. Phys. Lett.* **2008**, *92*, 151504. [[CrossRef](#)]
14. Stoffels, E.; Flikweert, A.J.; Stoffels, W.W. Plasma needle: A non-destructive atmospheric plasma source for fine surface treatment of (bio) materials. *Plasma Sources Sci. Technol.* **2002**, *11*, 383–388. [[CrossRef](#)]
15. Országh, J.; Skalný, J.D.; Mason, N.J. Ozone Formation in a Coaxial DC Corona Discharge under Carbon Dioxide Gas Flow. *Plasma Process. Polym.* **2007**, *4*, 694–700. [[CrossRef](#)]
16. Chen, J.; Wang, P. Effect of Relative Humidity on Electron Distribution and Ozone Production by DC Coronas in Air. *IEEE Trans. Plasma Sci.* **2005**, *33*, 808–812. [[CrossRef](#)]
17. Ben Gadoria, R.; Roth, J.R.; Montie, T.C.; Kelly-Winterberg, K.; Tsai, P.; Helfritsch, D.J.; Feldman, P.; Sherman, D.M.; Karakaya, F.; Chen, Z. Sterilization and plasma processing of room temperature surfaces with a one atmosphere uniform glow discharge plasma (OAUGDP). *Surf. Coat. Technol.* **2000**, *131*, 528–541. [[CrossRef](#)]
18. Barillas, L. Design of a Prototype of Water Purification by Plasma Technology as the Foundation for an Industrial Wastewater Plant. *J. Phys. Conf. Ser.* **2015**, *591*, doi:10–1088. [[CrossRef](#)]
19. Kuwahara, T. Fundamental characteristic of reduction of energy consumption in water sterilization using nonthermal plasma. In Proceedings of the 2017 IEEE Industry Applications Society Annual Meeting, Cincinnati, OH, USA, 1–5 October 2017; pp. 1–7. [[CrossRef](#)]
20. Kuwahara, T. Reduction in Energy Consumption Using Fuel Cells in Nonthermal Plasma-Based Water Sterilization by Bubbling Ozone. *IEEE Trans. Ind. Appl.* **2018**. [[CrossRef](#)]
21. Weltmann, K.-D.; Von Woedtke, T. Basic requirements for plasma sources in medicine. *Eur. Phys. J. Appl. Phys.* **2011**, *55*, 1–27. [[CrossRef](#)]
22. Hammadi, N.; Zegrar, M.; Nemnich, S.; Dey, Z.; Remaoun, S.; Naouel, B.; Tilmatine, A. Development of a high-voltage high-frequency power supply for ozone generation. *J. Eng. Sci. Technol.* **2006**, *11*, 755–767.
23. Cui, J.; Wei, S.; Li, X.; Zhu, J.; Yin, W. Design of a High Voltage Power Supply for Electrocurtain. In Proceedings of the 3rd International Conference on Machinery, Materials and Information Technology Applications, Qingdao, China, 28–29 November 2015; pp. 1805–1809. [[CrossRef](#)]
24. Hakki, A.; Sadikov, K.; Kashapov, N. High Frequency High Power Full Bridge Converter for Plasma Torches. *J. Phys. Conf. Ser.* **2017**, *789*, 1–4. [[CrossRef](#)]
25. Zhu, Z.; Gong, C.; Wang, Z.; Tian, X.; Li, Y.; Yang, S.; Fu, R.K.; Chu, P.K. A specially designed PLC-based high-voltage pulse modulator for plasma immersion ion implantation. *IEEE Trans. Plasma Sci.* **2010**, *38*, 3083–3088. [[CrossRef](#)]
26. Rossi, J.O.; Ueda, M.; Barroso, J.J. Pulsed power modulators for surface treatment by plasma immersion ion implantation. *Braz. J. Phys.* **2004**, *34*, 1565–1571. [[CrossRef](#)]
27. Davari, P.; Zare, F.; Ghosh, A.; Akiyama, H. High-voltage modular power supply using parallel and series configurations of Flyback converter for pulsed power applications. *IEEE Trans. Plasma Sci.* **2012**, *40*. [[CrossRef](#)]
28. Davari, P.; Zare, F.; Ghosh, A. A flexible solid-state pulsed power topology. In Proceedings of the 2012 15th International Power Electronics and Motion Control Conference, Novi Sad, Serbia, 4–6 September 2012. [[CrossRef](#)]
29. Davari, P.; Zare, F.; Blaabjerg, F. Investigating pulsed discharge polarity employing solid-state pulsed power electronics. *Electr. Power Compon. Syst.* **2015**, 1–9. [[CrossRef](#)]
30. Caughman, J.B.O.; Goulding, R.H.; Biewer, T.M.; Bigelow, T.S.; Campbell, I.H.; Caneses, J.; Diem, S.J.; Fadnek, A.; Fehling, D.T.; Isler, R.C.; et al. Plasma source development for fusion-relevant material testing. *J. Vac. Sci. Technol.* **2017**, *35*. [[CrossRef](#)]
31. Li, Y.; Moschopoulos, G. A Single-Phase Single-Stage AC-DC Stacked Flyback Converter with Active Clamp ZVS. In Proceedings of the 2018 IEEE Applied Power Electronics Conference and Exposition (APEC), San Antonio, TX, USA, 4–8 March 2018; pp. 2035–2041. [[CrossRef](#)]
32. Pérez-Nicoli, P.; Silveira, F. Maximum efficiency tracking in inductive power transmission using both matching networks and adjustable AC–DC converters. *IEEE Trans. Microw. Theory Tech.* **2018**, 1–11. [[CrossRef](#)]

33. Kant, P.; Singh, B. A Multi-Pulse AC-DC Converter Fed 5-Level NPC Inverter Based VCIMD. In Proceedings of the 2018 IEEMA Engineer Infinite Conference (eTechNxT), New Delhi, India, 13–14 March 2018. [[CrossRef](#)]
34. Ma, H.; Li, Y.; Chen, Q.; Zhang, L.; Xu, J. A Single-Stage Integrated Boost-LLC AC-DC Converter with Quasi-Constant Bus Voltage for Multi-channel LED Street-Lighting Applications. *IEEE J. Emerg. Sel. Top. Power Electron.* **2018**, 1–12. [[CrossRef](#)]
35. Gautam, S.; Gupta, R. Balanced Control of Multicell AC-DC Converter with Cascaded H-bridge Cells. In Proceedings of the 2015 IEEE UP Section Conference on Electrical Computer and Electronics (UPCON), Allahabad, India, 4–6 December 2015. [[CrossRef](#)]
36. Lv, Z.; Xia, Y.; Chai, J.; Yu, M.; Wei, W. Distributed Coordination Control Based on State-of-Charge for Bidirectional Power Converters in a Hybrid AC/DC Microgrid. *Energies* **2018**. [[CrossRef](#)]
37. Salas-Puente, R.A.; Marzal, S.; González-Medina, R.; Figueres, E.; Garcera, G. Power Management of the DC Bus Connected Converters in a Hybrid AC/DC Microgrid Tied to the Main Grid. *Energies* **2018**. [[CrossRef](#)]
38. Yang, Y.; Wang, X.; Luo, J.; Duan, J.; Gao, Y.; Li, H.; Xiao, X. Multi-Objective Coordinated Planning of Distributed Generation and AC/DC Hybrid Distribution Networks Based on a Multi-Scenario Technique Considering Timing Characteristics. *Energies* **2017**. [[CrossRef](#)]
39. Pejmanfar, R.; Haghifam, M.R.; Soleymani, S.; Tavassoli, B. Large Signal Stabilization of Hybrid AC/DC Micro-Grids Using Nonlinear Robust Controller. *Energies* **2017**. [[CrossRef](#)]
40. Sathishkumar, P.; Krishna, T.N.V.; Khan, M.A.; Zeb, K.; Kim, H.J. Digital Soft Start Implementation for Minimizing Start Up Transients in High Power DAB-IBDC Converter. *Energies* **2018**. [[CrossRef](#)]
41. Barge, S.A.; Jagtap, S.R. Harmonic Analysis of Sinusoidal Pulse Width Modulation. *Int. J. Adv. Electr. Electron. Eng.* **2013**, 2, 13–16.
42. Namboodiri, A.; Wani, H.S. Unipolar and Bipolar PWM Inverter. *Int. J. Innov. Res. Sci. Technol.* **2014**, 237–243.
43. Farahani, H.F.; Sarabadani, H. Modulation index effect on the 5-level SHE-PWM voltage source inverter. *Engineering* **2011**, 3, 187. [[CrossRef](#)]



© 2018 by the authors. Licensee MDPI, Basel, Switzerland. This article is an open access article distributed under the terms and conditions of the Creative Commons Attribution (CC BY) license (<http://creativecommons.org/licenses/by/4.0/>).